

Title	Proton transport properties of poly (aspartic acid) with different average molecular weights
Author(s)	Nagao, Yuki; Imai, Yuzuru; Matsui, Jun; Ogawa, Tomoyuki; Miyashita, Tokuji
Citation	The Journal of Chemical Thermodynamics, 43(4): 613-616
Issue Date	2010-11-30
Type	Journal Article
Text version	author
URL	<a href="http://hdl.handle.net/10119/10629">http://hdl.handle.net/10119/10629</a>
Rights	NOTICE: This is the author's version of a work accepted for publication by Elsevier. Yuki Nagao, Yuzuru Imai, Jun Matsui, Tomoyuki Ogawa, Tokuji Miyashita, The Journal of Chemical Thermodynamics, 43(4), 2010, 613-616, <a href="http://dx.doi.org/10.1016/j.jct.2010.11.016">http://dx.doi.org/10.1016/j.jct.2010.11.016</a>
Description	

**Proton transport properties of poly(aspartic acid)  
with different average molecular weights**

Yuki Nagao<sup>a</sup>, Yuzuru Imai<sup>b</sup>, Jun Matsui<sup>c</sup>, Tomoyuki Ogawa<sup>d</sup>, Tokuji Miyashita<sup>c</sup>

<sup>a</sup>Department of Mechanical Systems and Design, Graduate School of Engineering, Tohoku University, 6-6-01 Aoba Aramaki, Aoba-ku, Sendai 980-8579, Japan

<sup>b</sup>Institute of Development, Aging and Cancer (IDAC), Tohoku University, 4-1 Seiryō-cho, Aoba-ku, Sendai 980-8575, Japan

<sup>c</sup>Institute of Multidisciplinary Research for Advanced Materials (IMRAM), Tohoku University, 2-1-1 Katahira, Sendai 980-8577, Japan

<sup>d</sup>Department of Electronic Engineering, Graduate School of Engineering, Tohoku University, 6-6-05 Aoba Aramaki, Aoba-ku, Sendai 980-8579, Japan

email: y\_nagao@energy.mech.tohoku.ac.jp

**Abstract**

We synthesized seven partially protonated poly(aspartic acids)/sodium polyaspartates (P-Asp) with different average molecular weights to study their proton transport properties. The number-average degree of polymerization (DP) for each P-Asp was 30 (P-Asp30), 115 (P-Asp115), 140 (P-Asp140), 160 (P-Asp160), 185 (P-Asp185), 205 (P-Asp205) and 250 (P-Asp250). The proton conductivity depended on the number-average DP. The maximum and minimum proton conductivities under a relative humidity of 70 % and 298 K were  $1.7 \times 10^{-3}$  (P-Asp140) and  $4.6 \times 10^{-4}$  S cm<sup>-1</sup> (P-Asp250), respectively. Differential thermogravimetric

analysis (TG-DTA) was carried out for each P-Asp. The results were classified into two categories. One exhibited two endothermic peaks between 270 and 300 °C, the other exhibited only one peak. The P-Asp group with two endothermic peaks exhibited high proton conductivity. The high proton conductivity is related to the stability of the polymer. The number-average molecular weight also contributed to the stability of the polymer.

Keywords: proton conduction, effect of molecular weight, poly(aspartic acid)

## **1. Introduction**

The design of highly proton conductive solid electrolytes is essential to many applications in the field of solid state ionics. One of the fundamental methods to make highly proton conductive material is chemical modification. The properties of chemical stability and mechanical strength are often unfavorable when obtained using chemical modifications such as sulfonation; however, proton conductivities exhibit excellent values. Due to such a trade off relationship between proton conductivity, mechanical strength, and chemical stability, a new method to make highly proton conductive material has been needed for a long time.

Recently, we have been reported a several proton conductive membranes based on oligomeric amides and polypeptide [1-4]. The thin films (~60 nm) of oligomers or polypeptide exhibit about 10 times higher proton conductivity than their pelletized sample (thickness about ~1 mm). Although the reason for this improvement in proton conduction remains unknown, application of this phenomenon shows promise of a new method to produce highly proton-conductive material.

Amino acid homopolymers, which have peptide linkages, have been known to exhibit interesting biochemical properties. Poly(aspartic acid) has free carboxylic acid groups on the

side chains. The electrical conductivity of a partially protonated poly(aspartic acid)/sodium polyaspartate (P-Asp) strongly depends on the relative humidity (RH), and the proton in P-Asp can move in the polymer [4]. However we observed that the proton conductivity was enhanced by the synthesis of the thin films in the previous study, the effect of molecular weight on the proton conductivity is not investigated yet. In the case of the Li ion conductivity, the effect of molecular weight on Li ion mobility in the system of poly(ethylene oxide)–LiCF<sub>3</sub>SO<sub>3</sub> electrolytes has been already reported in 1993 [5]. Shi *et al.* investigated Li ion mobility in poly(ethylene oxide) hosts with molecular weights ranging from 400 to  $4 \times 10^6$ , using electrochemical and pulsed field gradient NMR techniques. However the molecular weight dependence of the Li ion conductivity has been already reported [5,6], the effects of the molecular weight on the proton conductivity in the case of the proton conductive polymers were not sufficiently studied. In this paper, we investigate the proton transport properties of P-Asp with different average molecular weights.

## 2. Experimental

We carried out P-Asp synthesis as shown in Scheme 1. Table 1 summarizes the synthetic conditions for P-Asp with different number-average degree of polymerization (DP). P-Asp30, P-Asp160, P-Asp185, P-Asp205 and P-Asp250 were synthesized according to synthetic method A. The others (P-Asp115 and P-Asp140) were synthesized according to synthetic method B. The difference in synthetic methods A and B was due to the difference in the synthetic routes to polysuccinimide, as shown in Scheme 1. D, L-aspartic acid, *o*-phosphoric acid, mesitylene and sulfolane of reagent grades were commercially available and used without further purification. In synthetic method A, we added D, L-aspartic acid and 85 % *o*-phosphoric acid, as a catalyst, to a round bottom flask and mixed them for 10 minutes under

an Ar atmosphere. The mixture was heated at each temperature and reaction time shown in Table 1. In synthetic method B, we charged a four-neck, round bottom flask equipped with a Dean-Stark trap with a reflux condenser, a mechanical stirrer, a thermometer and an Ar inlet with D, L-aspartic acid, mesitylene, sulfolane and 85 % *o*-phosphoric acid under an Ar atmosphere. The mixture was refluxed under each temperature and reaction time as shown in Table 1.

The product was washed with methanol and water. The residue was washed with methanol and dried under reduced pressure. We added the dried sample and a solution of sodium hydroxide with deionized water to a stirred beaker under each hydrolysis condition, as shown in Table 1. After the reaction, the pH of the solution was adjusted to ~6 by the addition of 35 % aqueous HCl. A white precipitate was obtained by adding methanol. The sample was washed with methanol, and the centrifuge technique was used in the washing and separation procedures. The obtained sample was dried under reduced pressure. In the synthesis of P-Asp160 and P-Asp185, we observed the supernatant (P-Asp160) during the centrifuge technique. In the synthesis of P-Asp205 and P-Asp250, we settled the beaker containing the white precipitate for a while. The solution with the precipitate was divided between the upper layer (P-Asp205) and the lower layer (P-Asp250) in the beaker. Each precipitate was washed with methanol, and the centrifuge technique was used. The degrees of protonation of all P-Asp were ~10 %, a result that we checked by the titrimetric method.

The quality of the sample was checked by the  $^1\text{H}$  NMR measurements. The  $^1\text{H}$  NMR spectra in deuterium oxide, using Sodium 3-(trimethylsilyl)propionate-2,2,3,3-d<sub>4</sub> (TSP) as an internal reference, were obtained on an ECA-600 (JEOL) operated at 14 T. The average DP was determined by comparing, in the  $^1\text{H}$  NMR spectrum, the ratio of the peak area derived from the proton (3.9 – 4.2 ppm) of –CH at the amino end groups to the proton (2.5 – 3.2 ppm)

of the intrachain  $-\text{CH}_2$  and  $-\text{CH}_2$  at the carboxyl end groups. The average DP for P-Asp250 could not be determined because the peaks due to the protons of  $-\text{CH}_2$  and  $-\text{CH}$  at the amino end group were not clearly observed due to the low signal to noise ratio. Therefore, we determined the average DP for P-Asp250 by gel electrophoresis. P-Asp250 was transferred electrophoretically onto Ready-Gel J Peptide Gell (BIO-RAD) and visualized by staining with Coomassie brilliant blue R-350 (GE Healthcare) and Stains All Gel Staining kit AK02 (Primary Cell Co., Ltd.). SDS-PAGE Molecular Weight Standards, Low Range (BIO-RAD) was used at lane 1. A densitometric analysis to calculate the number-average molecular weight from the result of gel electrophoresis was carried out using Image J software from the US National Institute of Health.

Impedance measurements of the pelletized sample were carried out in the RH range of 50 – 70 % with a Solartron 1260 Impedance/Gain-Phase analyzer and a 1296 Dielectric Interface system. The RH and temperature were controlled with an Espec Corp. SH-221 humidity- and temperature-controlled chamber. The samples were processed into pellets of 2.5 mm diameter under pressures of  $\sim 1$  GPa, and porous gold paint (SILBEST No. 8560, Tokuriki Chemical Research) was used for electrodes.

Thermal properties of P-Asp were determined by a Rigaku Thermo plus TG 8120 under the following conditions: starting temperature, 30 °C; sample crucible, aluminum; sample weight,  $\sim 3$  mg; heating rate, 10 °C  $\text{min}^{-1}$ ; atmosphere,  $\text{N}_2$ ; flow rate, 100 mL  $\text{min}^{-1}$ . The sample was stored under an RH of 50 % and 25 °C before the measurements.

### **3. Results and Discussion**

#### *3.1. Characterization*

Figure 1 shows the  $^1\text{H}$  NMR spectra of P-Asp30 and P-Asp250. The broad peak width suggests that the sample is a polymer. The peak suggested by the asterisk in Fig. 1 is due to adsorbing methanol during synthesis procedure. All spectra of the samples were attributed to P-Asp, which reported in a previous study [4,7]. We did not observe any additional peaks, including the starting materials. The small peaks at 2.95 – 3.2 and 3.9 – 4.2 ppm in the spectrum of P-Asp30 were due to the protons of the  $-\text{CH}_2$  and  $-\text{CH}$  groups at the amino end groups, respectively. We determined the number-average DP by comparing the ratio of the peak area derived from the protons (3.9 – 4.2 ppm) of  $-\text{CH}$  at the amino end groups to the protons (2.5 – 3.2 ppm) of the intrachain  $-\text{CH}_2$  and  $-\text{CH}_2$  at the carboxyl end groups [4]. The number-average DP for each P-Asp was 30 (P-Asp30), 115 (P-Asp115), 140 (P-Asp140), 160 (P-Asp160), 185 (P-Asp185) and 205 (P-Asp205). The DP of P-Asp250 was not determined from the NMR spectrum because the peaks due to the protons of  $-\text{CH}_2$  and  $-\text{CH}$  groups at the amino end group were not clearly observed. This result suggested that the average DP of P-Asp250 was larger than that of P-Asp30. Therefore, we determined the number-average DP for P-Asp250 by gel electrophoresis as shown in Figure 2. P-Asp250 was not visualized with Coomassie brilliant blue R-350 but with Stains All Gel Staining kit AK02. The obtained band derived from P-Asp250 was broad. The number-average molecular weight and number-average DP were 34 kDa and 250 (P-Asp250), respectively.

Weight loss curves (TG) of all P-Asp were shown in Figure 3. The quantity of water molecules included in the polymer under an RH of 50 % and 25 °C is about one water molecule per unit (from the results of another measurement). Therefore, the weight loss from the starting temperature is due to the loss of water molecules in the polymer. The weight loss of P-Asp140, P-Asp160 and P-Asp185 at 150 °C was large compared to that of the other polymers.

### 3.2. Proton transport properties of P-Asp with different degree of polymerization

Figure 4 shows the dependence of the proton conductivity on the number-average DP. The resistance was directly given by the intersection of a depressed semicircle with the real axis in the complex plane impedance plots. The proton conductivity increased by three orders of magnitude with increase in RH from 50 to 70 %. Such a large dependence of proton conductivity on RH could arise from the proton conduction paths developed by water uptake. The proton conductivity depended on the DP in the RH range of 50 – 70 %, especially at an RH of 50 %. The maximum proton conductivity yielded a DP of around 140. The difference between the maximum and minimum proton conductivities was more than one order of magnitude at an RH of 50 %. The maximum and minimum proton conductivities were  $1.7 \times 10^{-3}$  (P-Asp140) and  $4.6 \times 10^{-4}$  S cm<sup>-1</sup> (P-Asp250), respectively, with an RH of 70 % and 298 K.

Figure 5 shows the DTA curves of all P-Asp. The results were classified into two categories. The DTA curves of P-Asp30, P-Asp115, P-Asp205 and P-Asp240 possessed one endothermic peak at 289 – 290 °C. The others (P-Asp140, P-Asp160 and P-Asp185) had two endothermic peaks between 270 and 300 °C. These first reactions occurred below 289 °C. These results suggested that P-Asp140, P-Asp160 and P-Asp185 were more unstable polymers than the others.

Figure 6 shows the relationship between the first reaction temperature from the DTA curve and the proton conductivity at each DP. While the first reaction temperature was low around a DP of 160, the proton conductivity increased around a DP of 140. The high proton conductivity could relate to the stability of the polymer, which depended on the number-average DP. Other effects for increasing the proton conductivity should be considered



because P-Asp115 which possessed one endothermic peak exhibited relatively high proton conductivity.

#### **4. Conclusions**

In order to study the proton transport properties of partially protonated poly(aspartic acids)/sodium polyaspartates (P-Asp) with different average molecular weights, we synthesized seven P-Asp with different number-average DP. The number-average DP for each P-Asp was 30 (P-Asp30), 115 (P-Asp115), 140 (P-Asp140), 160 (P-Asp160), 185 (P-Asp185), 205 (P-Asp205) and 250 (P-Asp250). The proton conductivity depended on the number-average DP. The maximum and minimum proton conductivities under a relative humidity of 70 % and 298 K were  $1.7 \times 10^{-3}$  (P-Asp140) and  $4.6 \times 10^{-4}$  S cm<sup>-1</sup> (P-Asp250), respectively. Differential thermogravimetric analysis (TG-DTA) was checked for each P-Asp. The results were classified into two categories. One group exhibited two endothermic peaks between 270 and 300 °C, and the other displayed only one peak. P-Asp with two endothermic peaks exhibited high proton conductivities. A high proton conductivity is related to the stability of the polymer. The number-average molecular weight could also contribute to the stability of polymer.

#### **Acknowledgements**

The authors thank Ms. M. Sasaki for helping with the synthesis procedure and Primary Cell Co., Ltd., Japan for supply of Stains All Gel Staining kit AK02. This study was supported by the Program for Improvement of Research Environment for Young Researchers from Special Coordination Funds for Promoting Science and Technology (SCF)

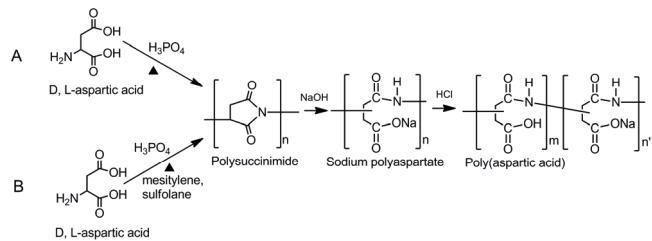
commissioned by the Ministry of Education, Culture, Sports, Science and Technology (MEXT) of Japan.

## References

- [1] Y. Nagao, N. Naito, F. Iguchi, N. Sata, H. Yugami, *Solid State Ionics* 180 (2009) 589-591.
- [2] Y. Nagao, N. Naito, F. Iguchi, N. Sata, H. Yugami, *e-Journal of Surface Science and Nanotechnology* 7 (2009) 530-532.
- [3] Y. Nagao, M. Ando, H. Maekawa, C.H. Chang, F. Iguchi, N. Sata, *ECS Transactions* 16 (2009) 401-406.
- [4] Y. Nagao, F. Iguchi, N. Sata, H. Yugami, *Solid State Ionics* 181 (2010) 207-210.
- [5] J. Shi, C.A. Vincent, *Solid State Ionics* 60 (1993) 11-17.
- [6] Z. Stoeva, I. Martin-Litas, E. Staunton, Y.G. Andreev, P.G. Bruce, *J. Am. Chem. Soc.* 125 (2003) 4619-4626.
- [7] K. Tabata, M. Kajiyama, T. Hiraishi, H. Abe, I. Yamato, Y. Doi, *Biomacromolecules* 2(4) (2001) 1155-1160.

***Scheme Caption***

Scheme 1: Chemical structure and reaction scheme (synthetic methods A and B) of partially protonated poly(aspartic acid)/sodium polyaspartate (P-Asp) from D, L-aspartic acid.



Scheme 1

***Table Caption***

TABLE 1 : Synthesis conditions for P-Asp. Two synthetic methods were carried out. P-Asp30, P-Asp160, P-Asp185, P-Asp205 and P-Asp250 were synthesized according to synthetic method A. P-Asp115 and P-Asp140 were synthesized according to synthetic method B.

TABLE 1

	Synthetic method	Temperature /°C	Time /h	Hydrolysis condition	Centrifugal condition
P-Asp30	A	130	3	r.t., 20 mins	7200 rpm, 5mins
P-Asp115	B	165 – 168	12	r.t., 20mins	9500 rpm, 5mins
P-Asp140	B	170	4.5	r.t., 5 mins	9500 rpm, 5mins
P-Asp160	A	170	7	0 °C, 30 mins	9500 rpm, 5mins
P-Asp185	A	170	7	0 °C, 30 mins	9500 rpm, 5mins
P-Asp205	A	175	36	0 °C, 40 mins	9500 rpm, 5mins
P-Asp250	A	175	36	0 °C, 40 mins	9500 rpm, 5mins

### ***Figure Captions***

Fig. 1.:  $^1\text{H}$  NMR spectra of P-Asp30 and P-Asp250. The peak suggested by the asterisk is due to methanol.

Fig. 2: Lane 1, molecular mass standard, with the mass indicated on the left in the figure; lane 2, P-Asp250. Densitometric analysis revealed a peak position of P-Asp250 size distribution. The arrow indicates the position of the number-average molecular weight of P-Asp250.

Fig. 3: Weight loss curves (TG) of all P-Asp. ○: P-Asp30; □: P-Asp115; ●: P-Asp140; ■: P-Asp160; ▲: P-Asp185; +: P-Asp205; ×: P-Asp250.

Fig. 4: Dependence of the proton conductivity on number-average DP. ●: RH = 70 %; ■: RH = 60 %; ▲: RH = 50 %.

Fig. 5: DTA curves of all P-Asp. The upper direction along the vertical line is exothermic.

Fig. 6: Relationship between the first reaction temperature and proton conductivity at each DP. ■: the first reaction temperature from the results of the DTA curves; ●: Log (proton conductivity) under an RH of 50 % and 298 K.



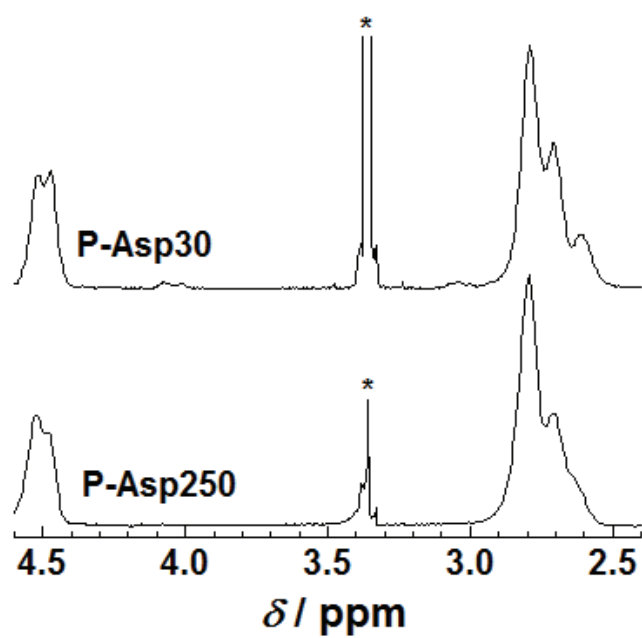


Fig. 1

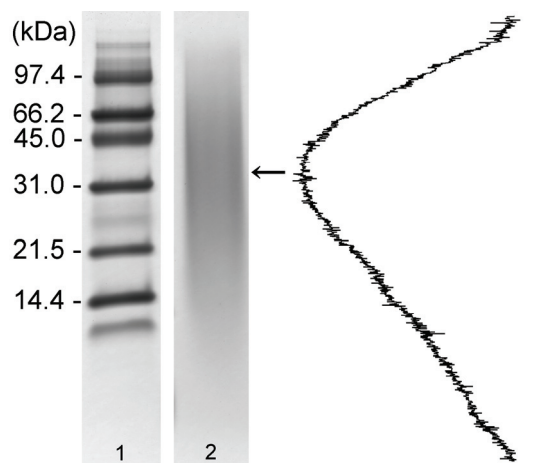


Fig. 2

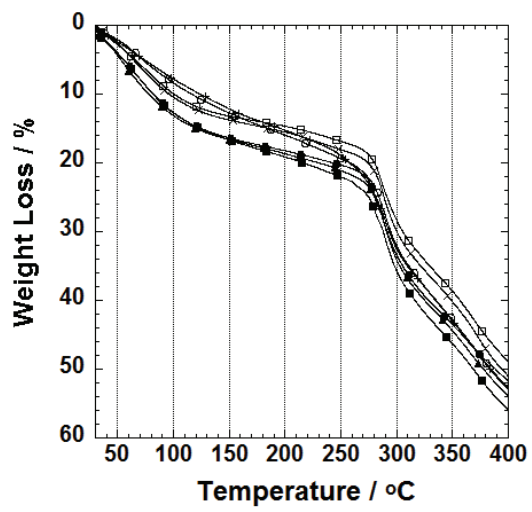


Fig. 3

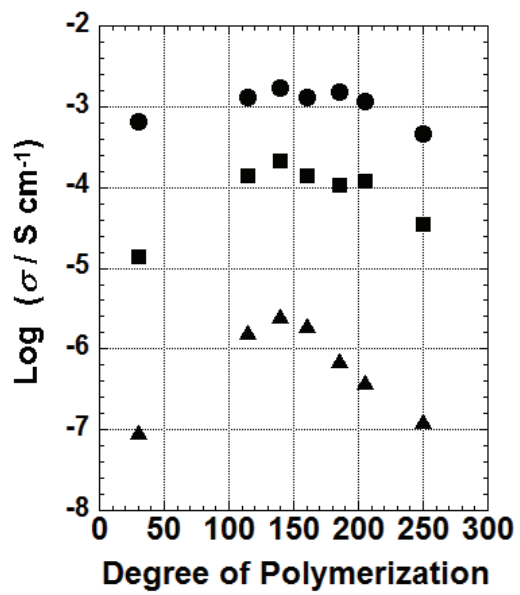


Fig. 4

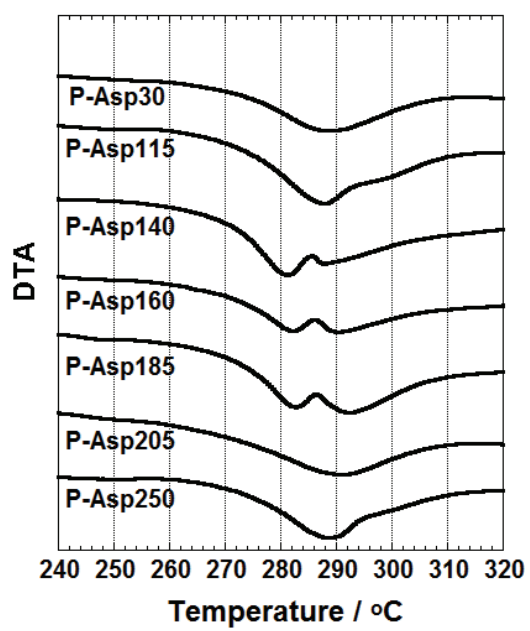


Fig. 5

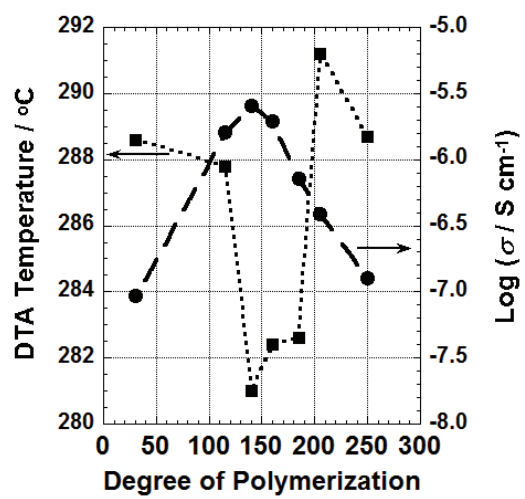


Fig. 6